Cell Reports, Volume *28*

Supplemental Information

Mapping Brain-Wide Afferent Inputs of Parvalbumin-Expressing GABAergic Neurons in Barrel Cortex Reveals Local and Long-Range Circuit Motifs

Georg Hafner, Mirko Witte, Julien Guy, Nidhi Subhashini, Lief E. Fenno, Charu Ramakrishnan, Yoon Seok Kim, Karl Deisseroth, Edward M. Callaway, Martina Oberhuber, Karl-Klaus Conzelmann, and Jochen F. Staiger

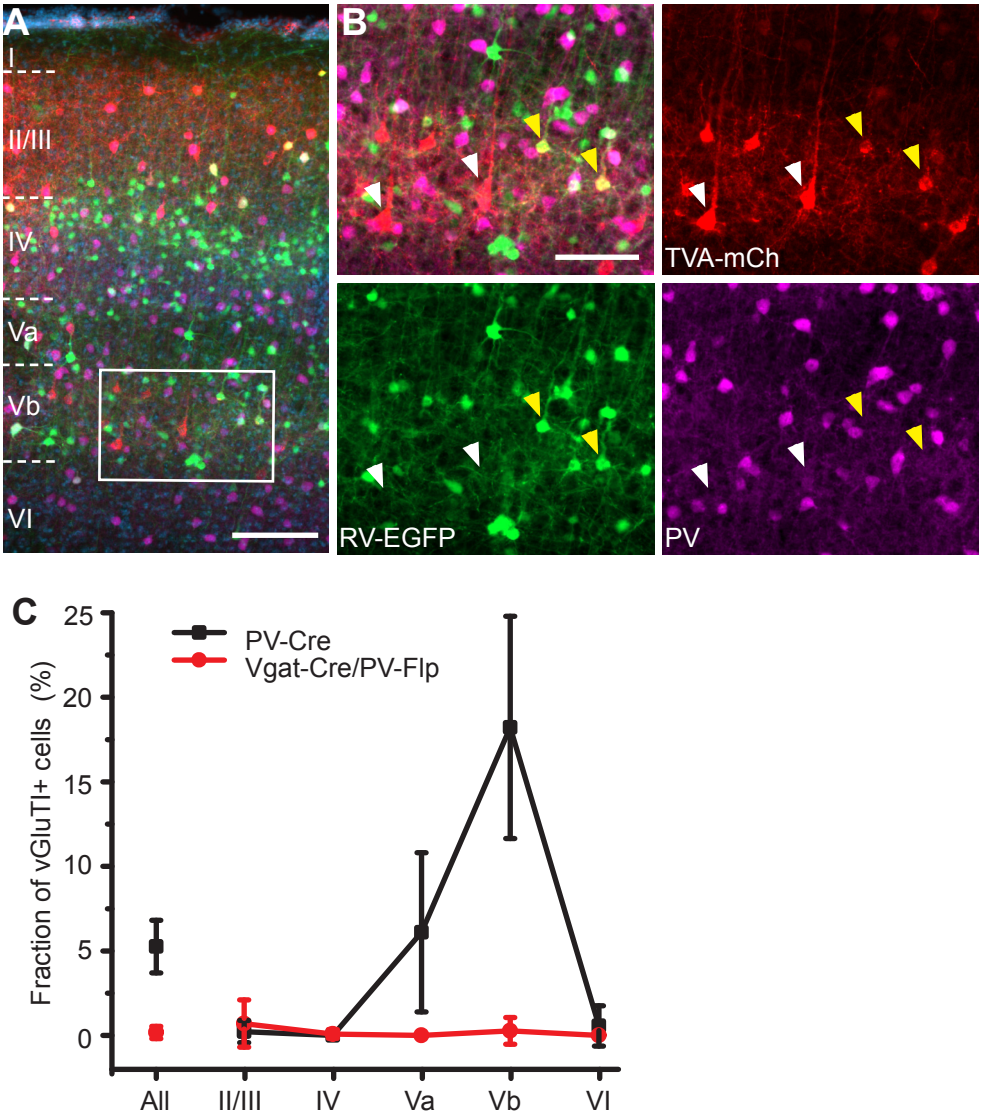

Figure S1: RV tracing in PV-Cre line includes excitatory starter cells (related to Figure 1)

(A) Injection of Cre-dependent helper viruses AAV-FLEX-TVA-mCherry and AAV-FLEX-oG, followed by RV-EGFP into PV-Cre mouse revealed a reliable transduction of pyramidal-shaped neurons in LV (scale bar: 200 µm).

(B) Insert in A. White arrowheads mark pyramidal-shaped, PV-immunonegative cells that express TVA-mCherry, probably due to a low-level expression of PV protein sufficient to activate Cre. Yellow arrowheads mark cells that additionally took up RV and are potential excitatory starter cells (scale bar: 50 µm).

(C) Fraction of excitatory marker vGluT1-RNA positive cells among all tdTomato-labeled cells in the PV-Cre/tdTomato and Vgat-Cre/PV-Flp/tdTomato mouse line across layers (n = each line 2 mice, 8 sections). In the PV-Cre line about 10.8 ± 2.9% of tdTomato-positive cells in LV were also vGluT1 positive, while in the Vgat-Cre/PV-Flp line this excitatory marker was virtually absent.

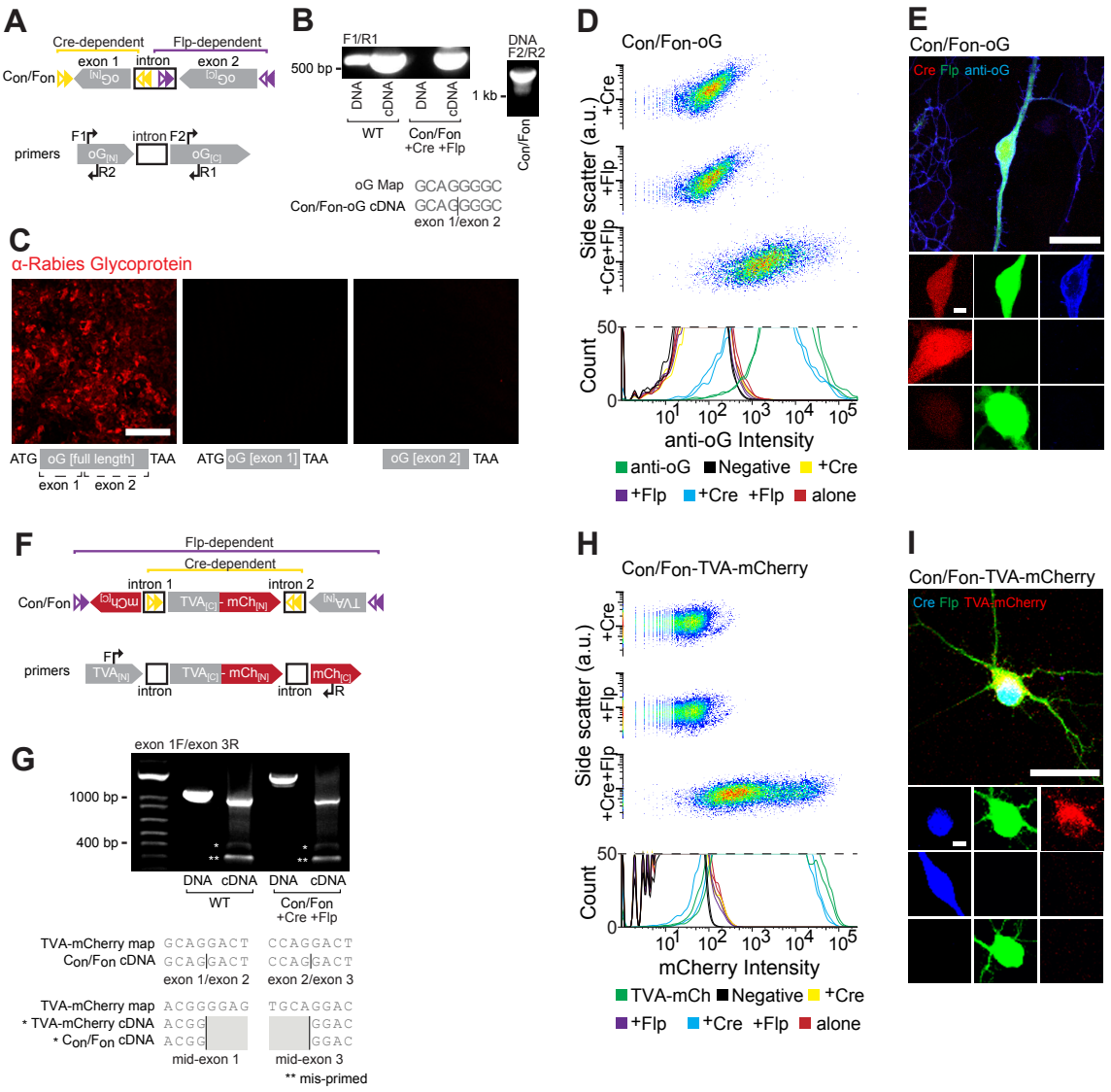

Figure S2: Engineering and validation of Cre- AND Flp-dependent Con/Fon-TVA-mCherry and Con/Fon-oG (related to Figure 1 and Method Details of STAR Methods)

(A) Molecular design (top) of Cre- (yellow) and Flp-dependent (purple) exons of oG (gray) created through the introduction of a central artificial intron (open box) and primers used for PCR and RT-PCR (bottom).

(B) PCR (lanes 1 and 3) and RT-PCR (lanes 2 and 4) using noted primers of wild-type oG (left) and Con/Fon-oG (right), showing expected band for Con/Fon-oG confirming proper exon re-orientation after recombinase activity and intron splicing. Splicing was further validated by sequencing of the Con/Fon-oG cDNA band (bottom). PCR of Con/Fon-oG DNA using primers recognizing the exons in the initial, reverse complement orientation gives a larger band including introns (right).

(C) Wildtype oG (left) but not fragments used for exon 1 or exon 2 (center, right) encodes functional rabies glycoprotein as assayed by antibody staining in HEK293 cells.

(D) Con/Fon-oG only encodes functional protein in the presence of both Cre and Flp while neither Cre nor Flp in isolation is sufficient to produce functional glycoprotein, as assayed by flow cytometry on HEK293 cells co-transfected with Con/Fon-oG and indicated recombinases.

(E) Cultured neurons express functional Con/Fon-oG (blue) only when co-transfected with Cre (red) and Flp (green) (scale bars: big panel: 50 μm, small panels: 5 μm).

(F) Molecular design (top) of Cre- (yellow) and Flp-dependent (purple) exons of TVA-mCherry created through the introduction of two introns (open boxes) and (bottom) primers used for PCR and RT-PCR.

(G) PCR (lanes 1 and 3) and RT-PCR (lanes 2 and 4) using noted primers of wild-type TVA-mCherry (left) and Con/Fon-TVA-mCherry (right), showing expected band for Con/Fon-TVA-mCherry cDNA and confirming proper exon re-orientation after recombinase activity and intron splicing. Splicing was further validated by sequencing of the WT- and Con/Fon-TVA-mCherry cDNA bands, including minor ones (bottom). The major band represents ideal splicing of the intron and recombinase components, while the smaller bands in both the wild-type and INTRSECT versions are either non-specific or represent inherent splicing separate from the introns introduced during INTRSECT molecular engineering.

(H) Con/Fon-TVA-mCherry only encodes functional protein in the presence of both Cre and Flp while neither Cre nor Flp in isolation is sufficient to produce functional protein, as assayed by flow cytometry on HEK293 cells co-transfected with Con/Fon-TVA-mCherry and indicated recombinases.

(I) Cultured neurons express functional Con/Fon-TVA-mCherry (red) only when co-transfected with Cre (blue) and Flp (green) (scale bars: big panel: 50 μm, small panels: 5 μm).

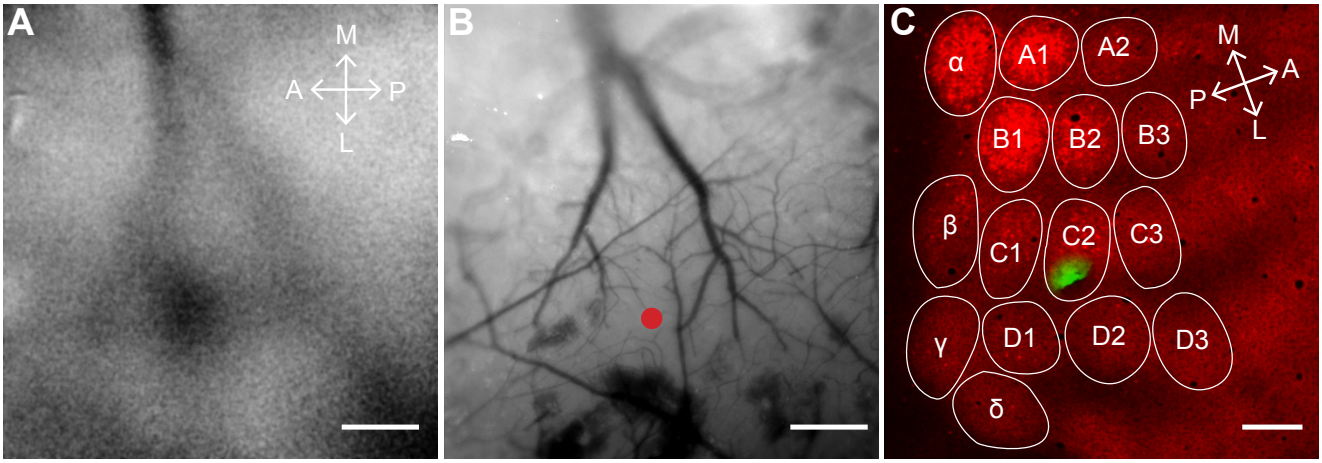

Figure S3: Mapping the C2 whisker representation in barrel cortex (related to Figure 3 and Method Details of STAR Methods)

(A) Average of 30 frames recorded 300 µm below exposed cortical surface. Repetitive whisker stimulation led to a localized change in blood flow, which induced a change in light reflectance visible as a dark dot.

(B) Surface vasculature was overlaid with image A and the location of the highest change in reflectance was marked with a red dot. The blood vessels were used as landmarks to guide the injection pipette.

(C) Tangential section through the barrel cortex of a Scnn1a-Cre/tdTomato mouse. Injection of DiO crystals was guided by the intrinsic signal elicited upon C2 whisker stimulation. This experiment demonstrated the accuracy of the injection procedure. (Scale bars: 200 µm)

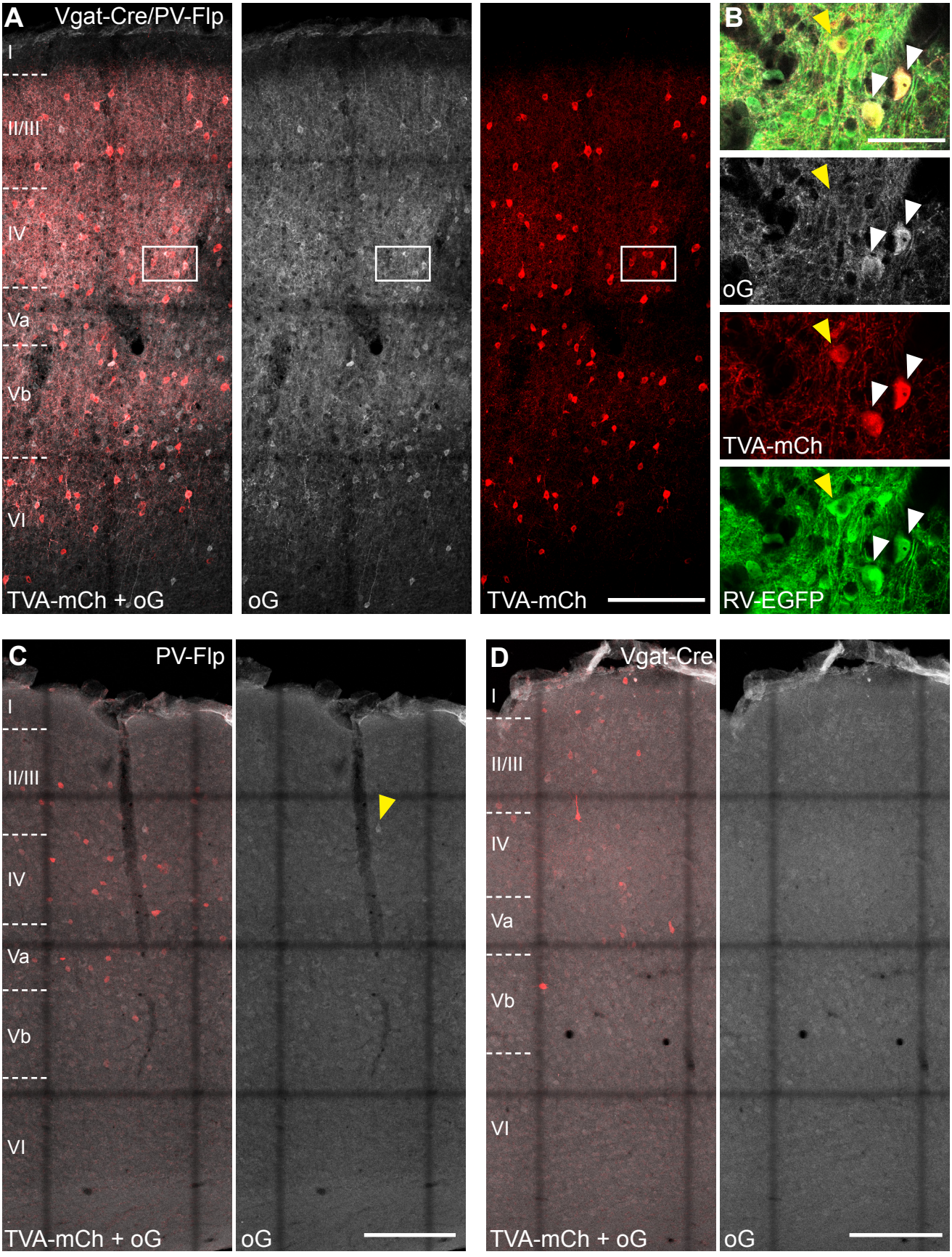

Figure S4: Antibody staining against optimized rabies glycoprotein (oG) (related to Figure 2)

(A) Coronal section through the barrel cortex of a PV-Flp and Vgat-Cre mouse after injection of AAV-TVA-mCh and AAV-oG followed by RV-EGFP. oG was labeled with antibody (gray; scale bar: 200 µm).

(B) Inserts of A show examples for TVA-mCherry, oG, EGFP triple labeled starter cells (white arrowheads) and an example for a TVA-mCherry, EGFP double labeled cell which lacks oG (yellow

arrowhead) and cannot serve as origin of transsynaptic spread (scale bar: 50 μm).

(C, D) Coronal section through the barrel cortex of a PV-Flp and Vgat-Cre mouse after injection of AAV-TVA-mCh and AAV-oG. While there was low-level recombinase-independent TVA-mCherry expression, immunolabeling for oG (gray) showed barely any signal. The yellow arrowhead marks a singular and exceptional oG positive cell in which recombinase-independent expression took place. Thus, oG expression solely occurs in the presence of Cre and Flp (scale bars: 200 μm).

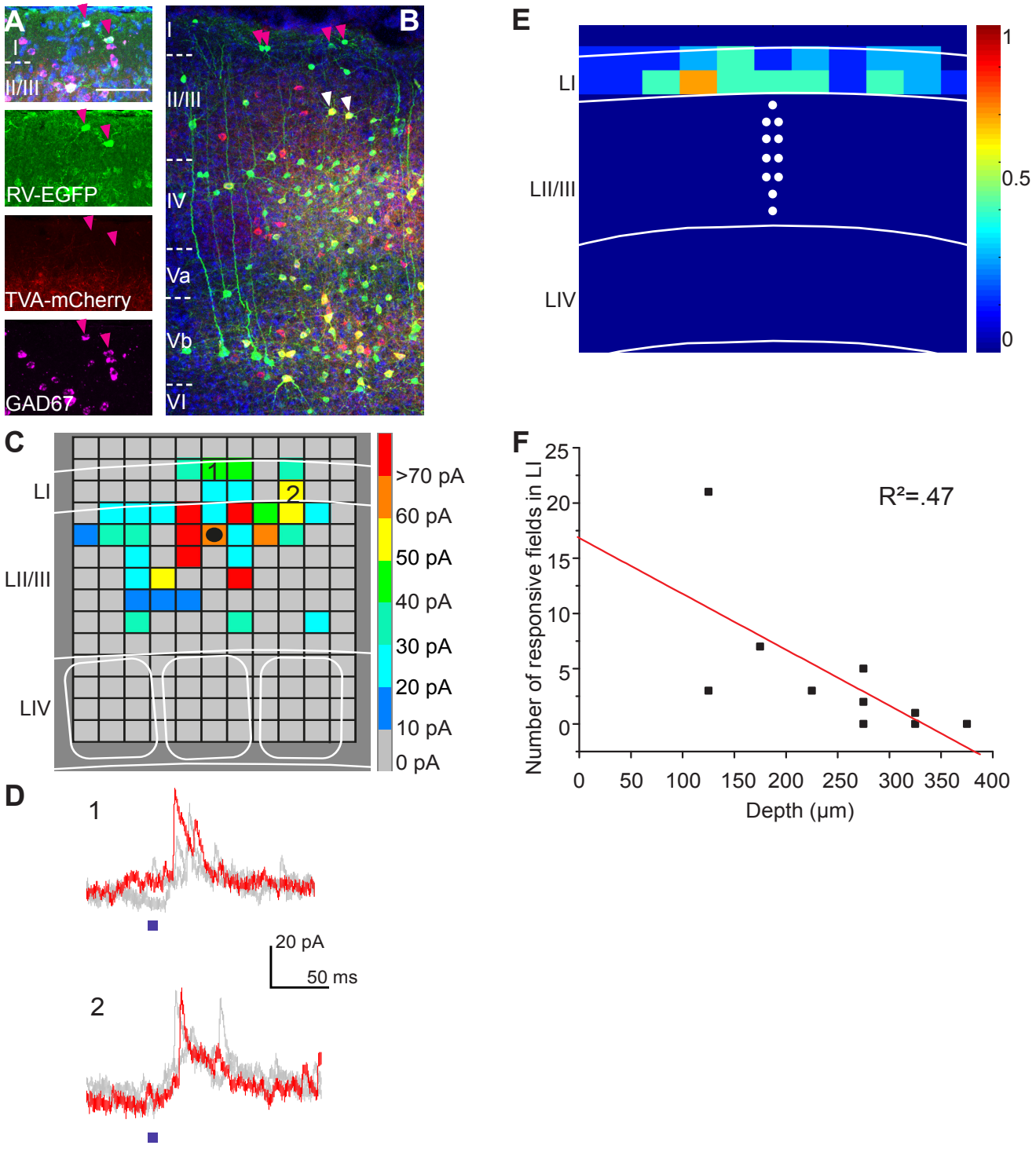

Figure S5: LI interneurons provide input to LII/III PV cells (related to Figure 4)

(A) RV-EGFP-labeled cells in LI at the injection site are all positive for GAD1 RNA, as demonstrated with FISH (n = 4 mice, 15 sections). Red arrowheads mark co-localized fluorescence.

(B) Cross-section through the injection site. Red arrowheads mark RV-EGFP-positive cells in LI, while white arrowheads mark starter cells in LII/III that could potentially be postsynaptic to LI neurons.

(C) Example map of synaptic responses onto one LII//III PV cell. Soma position is indicated by a black circle.

(D) Average postsynaptic responses recorded after triple photostimulation at the two squares indicated on map in C.

(E) Average map (n=10 cells) of postsynaptic responses onto PV cells elicited upon photostimulation in LI. Black circles mark the PV neurons' soma positions.

(F) Plot of PV cell soma depth below pial surface against the number of fields in LI whose photostimulation evoked a postsynaptic response in the PV cell.

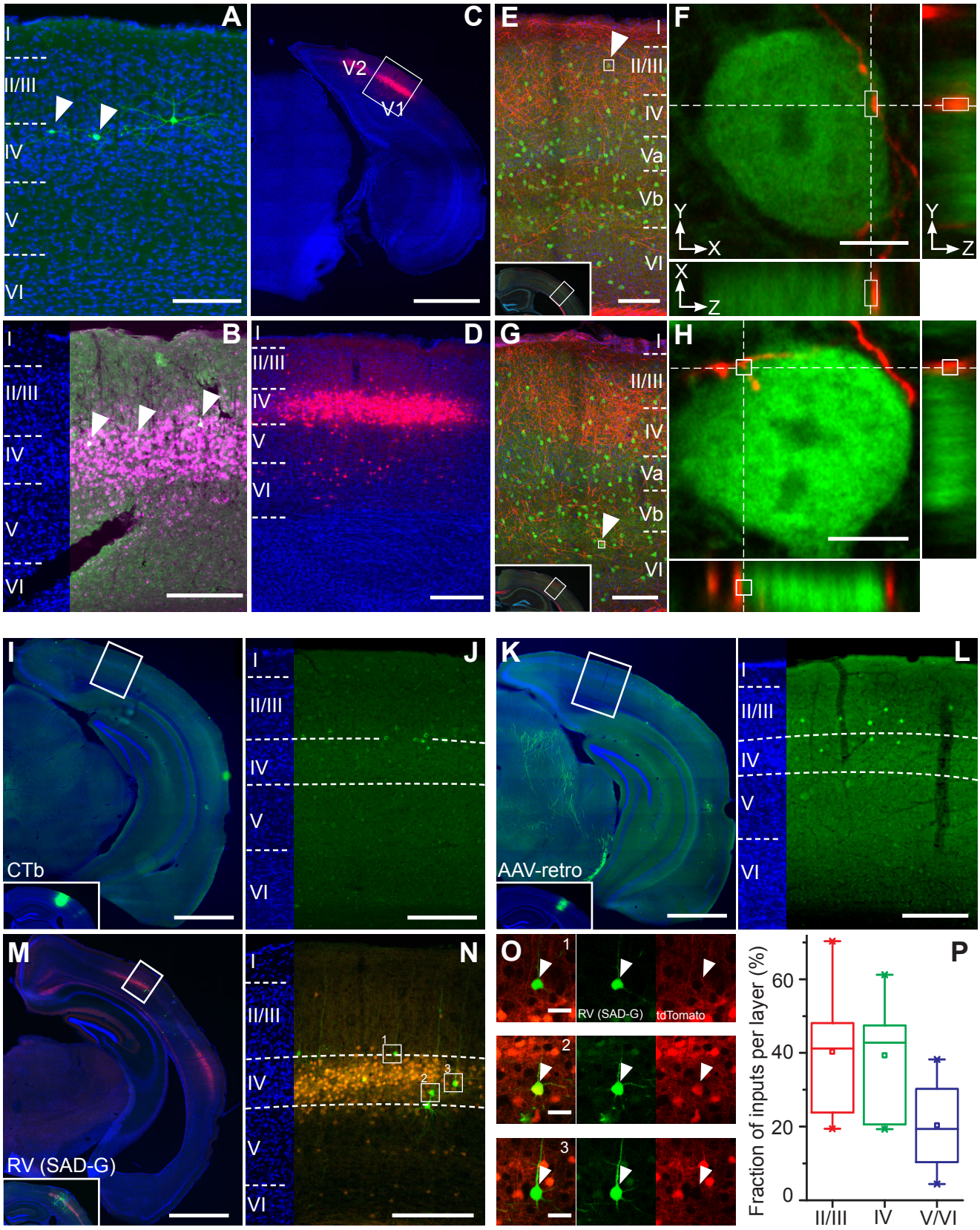

Figure S6: LIV neurons in visual cortex innervate PV cells in barrel cortex (related to Figure 6)

(A) Additional examples of transsynaptically labeled cells in visual cortex LIV (white arrowheads), which were often located at the border between LIII and LIV (scale bar: 200 µm).

(B) Staining for the LIV marker RorB in visual cortex revealed that putative transsynaptically labeled LIV projection neurons are well within the range of LIV cells, despite appearing at the LIII/IV boarder in DAPI staining (scale bar: 200 µm).

(C) Coronal section through visual cortex of LIV-specific mouse line Scnn1a-Tg3-Cre injected with AAV-FLEX-tdTomato (scale bar: 1000 μm).

(D) Insert of C. Close-up of injection site. LIV cells are strongly labeled but a few transduced LV/VI cells are visible, too (scale bar: 200 μm).

(E, G) Cross-sections through barrel cortex of injected animal in C/D, immuno-labeled for PV in green (scale bar: 100 μm).

(F, H) Inserts of E/G, respectively. tdTomato-positive axons originating from visual cortex were in close apposition to PV-stained cell bodies in barrel cortex. Boxes indicate the putative contact sites in the XY, XZ, and YZ planes (scale bar: 5 μm).

(I, K, M) Sections through visual cortex of mice injected with retrograde tracer CTb Alexa 488, AAV-retro-EGFP or RV-SADΔG-EGFP (SAD-G). Inserts show injection site in barrel cortex (scale bars: 1000 μm).

(J, L) Inserts of I/K respectively, showing retrogradely labeled projection neurons in visual cortex at higher magnification (scale bars: 200 μm).

(N, O) Insert of M showing cross-section through visual cortex of Scnn1a-Cre/tdTomato mouse injected with RV-SADΔG-EGFP (SAD-G). Single cell magnifications show a LIII/LIV-border cell non-co-localized with tdTomato (1), a tdTomato positive (2), and a tdTomato negative (3) LIV cell (scale bars: big insert 200 μm, small inserts 20 μm).

(P) Fraction of projection neurons in visual cortex by layer compartment. Neurons were retrogradely labeled by tracer injected in barrel cortex. LII/III and LIV contained an equal number of projection neurons.

Table S1: Average number of input cells in each input area (related to Figures 4, 5, 6)

Total inputs		3007
Total long-range inputs		407
Total subcortical long-range inputs		172
Ventral posteromedial nucleus of the thalamus		141
Posterior nucleus of the thalamus medial part		19
Basal forebrain		1
Other thalamic nuclei		8
Other subcortical structures		2
Total cortical long-range inputs		235
Barrel cortex	All	2600
	LI	70
	LII/III	375
	LIV	1209
	LVa	306
	LVb	478
	LVI	160
Secondary somatosensory cortex	All	140
	LII/III	22
	LIV	50
	LV	33
	LVI	34
Visual cortex	All	38
	LII/III	11
	LIV	22
	LV	3
	LVI	2
Auditory cortex	All	26
	LII/III	2
	LIV	11
	LV	8
	LVI	5
Primary somatosensory cortex body region	All	14
	LII/III	4
	LIV	3
	LV	5
	LVI	3
Motor cortex	All	9
	LII/III	4
	LV	4
	LVI	1
Other cortical stuctures	All	8

Table S2: List of oligonucleotides used in this study (related to Key Resources Table)

Oligonucleotide name	Primers	Resource
GAD1 riboprobe	Forward: CACAAACTCAGCGGCATAGA Reverse: GGACGAGCAACATGCTATGG	(Weissbourd et al., 2014)
RorB riboprobe	Forward: GGCACATACGCCAACGG Reverse: CGCAGCACAGTCAGGATTAAAGA	(Wagener et al., 2010)
SST riboprobe	Forward: CACAAACTCAGCGGCATAGA Reverse: GGACGAGCAACATGCTATGG	(Prönneke et al., 2015)
vGluT1 riboprobe	Forward: GCTGGCAGTGACGA AAGTGA Reverse: TGAGAGGGAAAGAGGGCTGG	(Prönneke et al., 2015)
VIP riboprobe	Forward: CTGTTCTCTCAGTCGCTGGC Reverse: GCTTTCTGAGGCGGGTGTAG	(Prönneke et al., 2015)
Con/Fon-oG (for RT and PCR)	Exon 1 Forward (1F): GCTATGAGGAAAGCCTGCAC Exon 1 Reverse (1R): GTGCAGGCTTTCCTCATAGC Exon 2 Forward (2F): AAGAGCGTGAGCTTCAGGAG Exon 2 Reverse (2R): CTCCTGAAGCTCACGCTCTT	This Publication
Con/Fon-TVA-mCherry (for RT and PCR)	Exon 1 Forward (1F):GTCAGTTCCGCTGCTCGGAG Exon 3 Reverse (3R): CTTGTACAGCTCGTCCATGC	This Publication